

AperTO - Archivio Istituzionale Open Access dell'Università di Torino

Combining label-free and fluorescence operation of Bloch surface wave optical sensors

This is the author's manuscript

Original Citation:

Availability:

This version is available <http://hdl.handle.net/2318/151984> since 2016-06-28T16:13:35Z

Published version:

DOI:10.1364/OL.39.002947

Terms of use:

Open Access

Anyone can freely access the full text of works made available as "Open Access". Works made available under a Creative Commons license can be used according to the terms and conditions of said license. Use of all other works requires consent of the right holder (author or publisher) if not exempted from copyright protection by the applicable law.

(Article begins on next page)

This is the author's final version of the contribution published as:

A. Sinibaldi; A. Fieramosca; R. Rizzo; O. Anopchenko; N. Danz; P. Munzert; C. Magistris; C. Barolo; F. Michelotti, Combining label-free and fluorescence operation of Bloch surface wave optical sensors, *Optics Letters*, 39, 10, 2014, pagg. 2947-2950, doi: 10.1364/OL.39.002947

The publisher's version is available at:

<https://www.osapublishing.org/ol/abstract.cfm?uri=ol-39-10-2947>

When citing, please refer to the published version.

Link to this full text:

<http://hdl.handle.net/2318/151984>

This full text was downloaded from iris-AperTO: <https://iris.unito.it/>

Combining label-free and fluorescence operation of Bloch surface wave optical sensors

Alberto Sinibaldi,¹ Antonio Fieramosca,¹ Riccardo Rizzo,¹ Aleksei Anopchenko,¹ Norbert Danz,² Peter Munzert,² Claudio Magistris,³ Claudia Barolo,³ and Francesco Michelotti^{1,*}

¹SAPIENZA University of Roma, Department of Basic and Applied Sciences for Engineering, Via A. Scarpa 16, 00161, Roma, Italy

²Fraunhofer Institute for Applied Optics and Precision Engineering IOF, A.-Einstein-St. 7, 07745, Jena, Germany

³University of Torino, Department of Chemistry and NIS Interdepartmental Centre, Via P. Giuria 7, 10125 Torino, Italy

*Corresponding author: francesco.michelotti@uniroma1.it

Received Month X, XXXX; revised Month X, XXXX; accepted Month X, XXXX; posted Month X, XXXX (Doc. ID XXXXX); published Month X, XXXX

We report on the design, fabrication and characterization of optical sensors based on Bloch surface waves propagating at the truncation edge of one dimensional photonic crystals. The sensors can be simultaneously operated in both a label-free mode, where small refractive index changes at the surface are detected, and a fluorescence mode, where the fluorescence from a novel heptamethyne dye label in proximity of the surface is collected. The two modes operate in the near infrared spectral range with the same configuration of the optical reading apparatus. The limit of detection is shown to be smaller than that of equivalent surface plasmon sensors and the fluorescence collection efficiency is such that it can be efficiently analysed by the same camera sensor used for label-free operation. © 2014 Optical Society of America

OCIS Codes: : (240.6690) Surface waves; (050.5298) Photonic crystals; (230.5298) Photonic crystals; (130.6010) Sensors; (160.5293) Photonic bandgap materials; (170.6280), Spectroscopy, fluorescence and luminescence; (170.4580) Optical diagnostics for medicine.

Surface plasmon polaritons (SPP) are presently a standard in label-free optical biosensing [1-2]. Coupling to SPP also increases the brightness of labels in fluorescence microscopy, thanks to the increased excitation rates [3] and to channeling of the emission inside narrow angular cones [4]. However absorption losses in metals result in a broadening of the SPP resonances and limit both the label-free and the fluorescence operation. Therefore new more effective solutions are desired.

Recently it was shown that Bloch surface waves (BSW) sustained at the truncation interface of finite one dimensional dielectric photonic crystals (1D-PC) show characteristics similar to SPP and, due to their extremely reduced losses, can outperform them for label-free [5,6] and fluorescence [7] operation.

Here we report on the design, fabrication and characterization of sensing chips based on 1D-PC sustaining BSW and operating in the near infrared simultaneously in a label-free and a fluorescence mode on the same instrumental platform, showing increased resolution with respect to surface refractive index changes and high fluorescence collection efficiency.

The instrumental platform we used was previously developed for surface plasmon resonance (SPR) label-free biosensing and makes use of polymer substrates (TOPAS, $n_{\text{sub}}=1.526$) with micro-optical elements obtained by injection molding [8]. For SPR operation the substrates are coated with a gold layer with thickness in the range of 45 nm. As shown in Fig.1 (top), the reflectance is measured at $\lambda_0=804$ nm ($\Delta\lambda=2.5$ nm, spectrally filtered LED illumination) in the $\theta \in [63.2^\circ, 67.2^\circ]$ angular range above the total internal reflection (TIR) edge. In this work either ethanol (EtOH) or doubly deionized water (ddH₂O) is the external liquid ($n_{\text{EtOH}}=1.357$, $n_{\text{ddH}_2\text{O}}=1.328$ [9]) with

the TIR edge situated at $\theta_{\text{TIR}}=62.73^\circ$ or $\theta_{\text{TIR}}=60.87^\circ$, respectively.

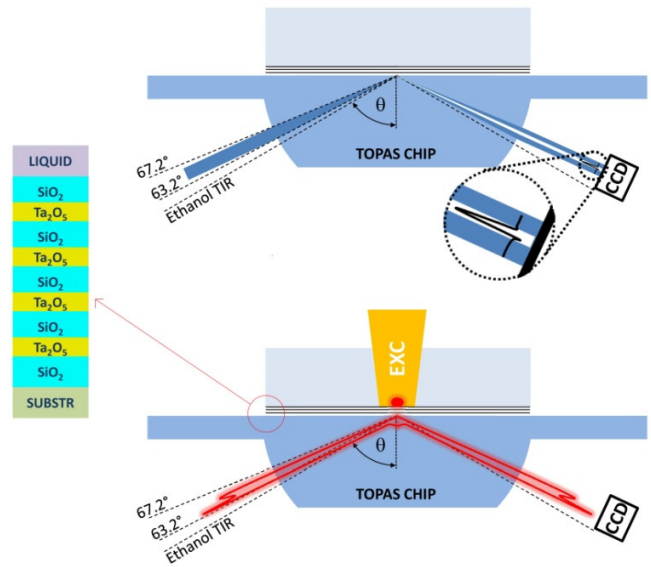


Fig. 1. Sketches of the label-free (top) and fluorescence (bottom) modes of operation of the sensing platform. (top) A focused beam at λ_0 is used to illuminate the chip under total internal reflection conditions and the presence of a resonance is detected by a CCD sensor. (bottom) An external laser beam at λ_{EXC} is used to excite molecules in proximity of the chip surface and the emission, strongly coupled to the BSW surface bound modes, is directed into a narrow angular range and detected by the same CCD sensor. (left) Sketch of the 1D-PC geometry used in the experiments (not to scale).

The 1D-PC used in the experiments were deposited on 170 μm thick microscope cover slides (Menzel Gläser) by plasma ion assisted evaporation under high vacuum conditions using an APS904 coating system (Leybold Optics). SiO_2 and Ta_2O_5 were used as low and high index layers with complex refractive indices $n_L=1.454+j6\text{E-}6$ and $n_H=2.060+j2\text{E-}5$ at λ_0 , respectively.

Starting from n_L and n_H , we designed the thicknesses of the 1D-PC layers in order to obtain a BSW resonance inside the angular acceptance range of our optical reading system. As a result the 1D-PCs designed, fabricated and used in the experiments had the structure substrate / L(HL)^4 / EtOH with design thicknesses $d_H=170$ nm and $d_L=495$ nm. The last layer in the stack, which is in contact with the external liquid, is SiO_2 . The first L layer was deposited in order to provide a defined surface quality for the growth of the 1D-PC. The layers' deposition tolerance ($\pm 2\%$ thickness) ensures that the BSW resonance is within an angular range of 0.2° around the nominal angular position.

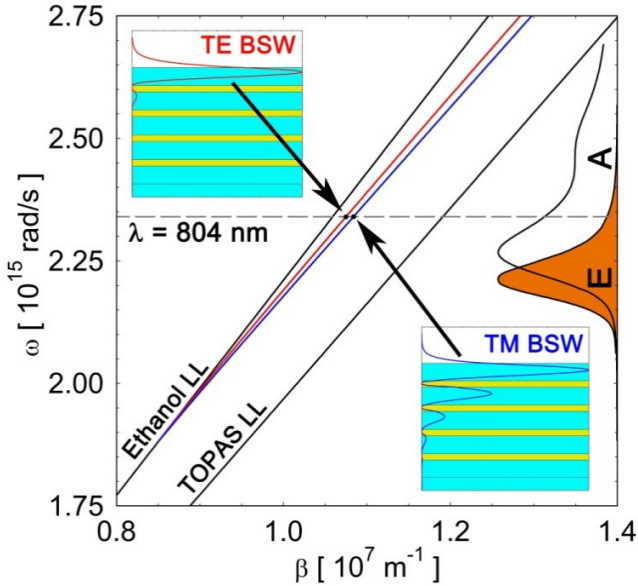


Fig.2. Dispersion relations $\omega(\beta)$ for the TE and the TM polarized BSW sustained in EtOH by the 1D-PC described in the text. For small ω the dispersions get to the light line in ethanol (Ethanol LL). (Insets) Normalized $|E|^2$ and $|H|^2$ transverse distributions for both modes. The absorption and emission spectra of the Cy7-VG20 dye used in the fluorescence experiments are also shown. The dashed line marks the wavelength λ_0 used for the label-free operation.

The peculiarity of the present design is that the 1D-PC sustains both a TE and a TM polarised BSW. Such condition cannot be achieved with SPP that are only TM polarized. In Fig.2 we show the dispersion relations for such TE (red) and TM (blue) modes calculated in EtOH by means of a transfer matrix method [10]. The dispersions are plotted in the (ω, β) plane where ω is the angular frequency and β is the wavevector projection along the 1D-PC surface; the (ω, β) window corresponds to $\lambda \in [700 \text{ nm}, 1000 \text{ nm}]$ and $\theta \in [62.8^\circ, 67.5^\circ]$. The

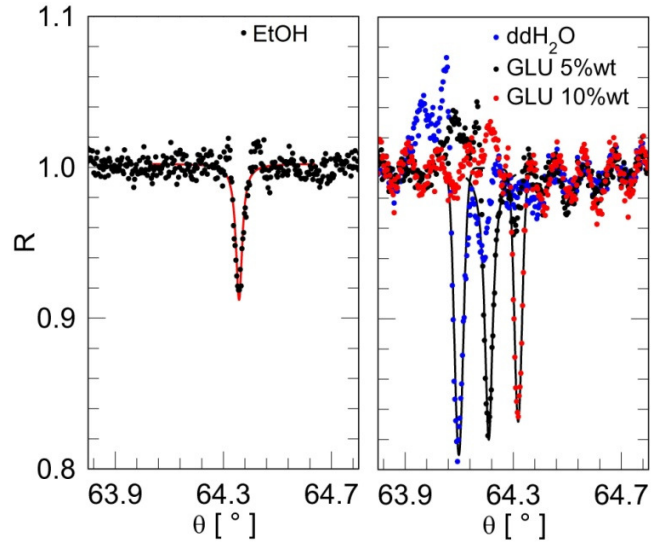


Fig.3. Label-free operation of the sensors at λ_0 . The solid lines are guides for the eye. For the sake of clarity, the plots are shown in a reduced angular interval with respect to that taken by the CCD. (left) BSW resonance measured in EtOH. (right) BSW resonance measured in ddH₂O (blue dots), 5%wt glucose in ddH₂O (black dots), 10%wt glucose in ddH₂O (red dots). The fringes in the measurement are due to interference in the glue layer between the TOPAS substrate and the cover slides.

dispersions always lay between the light lines in EtOH and TOPAS. The insets in Fig.2 illustrate that at λ_0 the BSW energy is confined close to the 1D-PC interface to the external medium. As a consequence, the modes' characteristics (effective index, losses, dispersion relation) are strongly sensitive to the properties of the external medium, making them very promising for label-free biosensing [6,11,12]. Moreover an emitter placed in proximity of the interface can couple very efficiently to such modes.

After fabrication the cover slides with the 1D-PC were adapted to a bare TOPAS chip by means of an index matching oil. The chip was previously thinned to account for the thickness of the cover slide when mounting on the instrumental platform, polished and topped with a glued 170 μm cover slide in order to prevent damage when using the oil. Alternatively the 1D-PC can be deposited directly on TOPAS chips [6].

Complete sensors were mounted on the instrument to carry out the test of the sensitivity with respect to changes of the external refractive index (label-free operation) and the efficiency to collect the emission of a dye in close proximity of the external interface (fluorescence operation).

For what is concerning the label-free operation, Fig.3 shows angular reflectance R spectra measured at λ_0 either in EtOH or in ddH₂O solutions, when the polarization is set to TE.

In ethanol environment the excitation of the TE BSW gives rise to a very narrow dip in the reflection spectrum of 9% (depth $D=0.09$) and a full width half maximum $W=0.030^\circ$. For comparison at the same λ_0 SPP show

resonances with $D = 0.76$ and $W = 1.47^\circ$ [6]. Here the small value for D is due to both the small absorption losses in the dielectric stack and the limited line-width $\Delta\lambda$ of the illumination system. When fitting the reflectance data one can retrieve the real thicknesses of the 1D-PC layers. We found: substrate / 485.0 nm / 165.0 nm / 496.8 nm / 173.1 nm / 501.5 nm / 174.2 nm / 492.5 nm / 167.8 nm / 486.5 nm / EtOH.

In the case of ddH₂O the light line is shifted to lower angles, the BSW resonance gets broader and the effect of the illumination line-width is reduced: therefore the BSW resonance is deeper with $D = 0.20$ and $W = 0.036^\circ$. In order to evaluate the volume sensitivity $S_V = d\theta / dn$, we poured onto the sensor's surface several solutions of glucose in ddH₂O with known concentrations $[C]$. In Fig.3 (right) we show the BSW resonance position for $[C] = 5\%$ wt (black dots) and $[C] = 10\%$ wt (red dots). Assuming that the refractive index change of the solution is related to the concentration by $\Delta n = \alpha * [C]$, with $\alpha = 1.5E-3$ RIU/% [13], we find that $S_V = 14.7^\circ / \text{RIU}$. For comparison SPP show $S_V = 92.7^\circ / \text{RIU}$ at the same λ_0 [6]. However, if we estimate the figure of merit defined as $\text{FoM} = S_V * D / W$ [1,6], that is inversely proportional to the limit of detection of the sensor (LoD), we find that $\text{FoM}_{\text{BSW}} = 82 \text{ RIU}^{-1}$. The comparison of such value with that found for SPP $\text{FoM}_{\text{SPP}} = 48 \text{ RIU}^{-1}$ [6] shows that, for this particular 1D-PC design, the LoD is about twice smaller. However preliminary studies not reported here indicate that the FoM can be further increased by optimizing the 1D-PC design and the angular detection window [14].

Concerning the fluorescence operation of the sensor, we decorated the surface with purposely selected dye molecules. With reference to Fig.1 (bottom) we excited the molecules by an external laser beam at λ_{exc} and collected the emission in the same angular range as in the label-free mode with the same CCD sensor (operated at a different gain and integration time). This condition is very similar to what one could have when performing an immuno-assay on top of such type of sensor [10] in which some of the antibodies are labeled with a fluorescent tag. As a dye we selected a cyanine molecule (see inset Fig. 4), namely Cy7-VG20, which shows an emission spectrum in a wavelength range that, via the BSW dispersion, corresponds to surface waves that can be outcoupled in the angular window of the instrument. In Fig.2 we show the absorption and emission spectrum of such a dye. Coupling of the emission to BSW makes that, for example, the peak emission wavelength $\lambda_{\text{peak}} = 837\text{nm}$ corresponds to $\beta = 2\pi\lambda_{\text{peak}} * n_{\text{sub}} * \sin(\theta) - 1.03E7 \text{ m}^{-1}$, i.e. to an angle $\theta \sim 64^\circ$ well in the window.

The Cy7-VG20 dye was prepared through a microwaves condensation of a quaternized 6-carboxybenz[e]indolenine with N-[5-Anilino-3-chloro-2,4-(propane-1,3-diyl)-2,4-pentadiene-1-ylidene]anilinium chloride [15], in presence of potassium acetate, in EtOH [16]. The obtained crystalline powder was characterized by Nuclear Magnetic Resonance and Mass Spectrometry.

For the fluorescence operation the sensors were topped with metal plate with a hole defining a cell located above the sensitive area. The plate was adapted to the surface by means of a VITON o-ring. For surface decoration the cell was filled with a 1mM solution of Cy7-VG20 in EtOH,

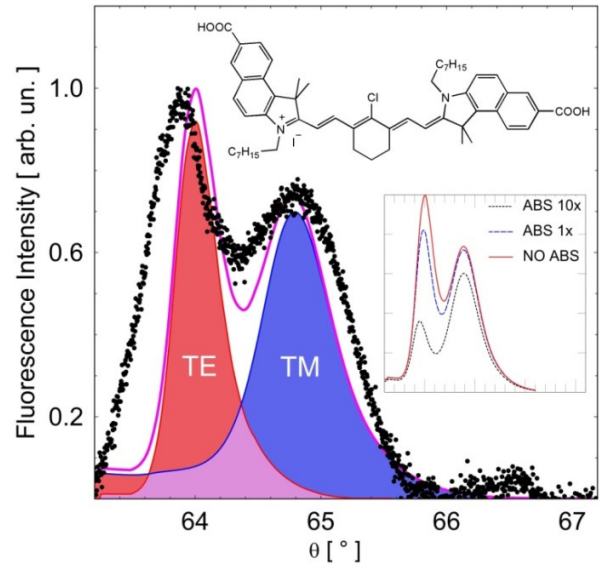


Fig.4. Experimentally measured angular distribution (dots) of the fluorescence intensity collected by the CCD sensor upon excitation of the Cy7-VG20 molecules by the external laser at λ_{exc} . The angular range is the same used for the label-free operation. The theoretical curve (solid purple curve) was calculated according to the procedure described in the text. The two TE (red) and TM (blue) are also plotted, respectively. (Top inset) Chemical structure of the Cy7-VG20 dye. (Bottom inset) Angular emission spectra calculated for three different absorption levels of Cy7-VG20 (the axes are the same of the main figure).

closed by a glass window and incubated overnight. Before decoration the sensor's surface was cleaned with a piranha solution for 10min. We tested by the label-free measurement that repeated (>50) piranha cleaning doesn't affect the BSW resonance characteristics, indicating that the 1D-PC geometry and optical quality are preserved (no etching of the last layer and no under-etching, no increase of surface scattering). After incubation the staining solution was removed from the pool that was then repetitively rinsed with pure EtOH.

At the end of the decoration procedure we filled the pool with pure EtOH and closed it with a glass plate. The transparent window allows an unfocused laser beam at $\lambda_{\text{exc}} = 632.8 \text{ nm}$ (He-Ne, 1mW at the surface) to reach the 1D-PC surface and excite the dye. In Fig.4 we show the angular distribution of the fluorescence collected by the CCD sensor (Sony ICX205AL) when the label-free illumination beam is switched off and the fluorescence excitation beam is switched on. The spectrum was collected with gain $G = 600$ and integration time 5.1 s; such values must be compared with those used for the label-free operation, $G = 374$ and $\tau = 1/15 \text{ s}$. The angular spectrum presents two peaks corresponding to the TE (smaller angles) and TM (larger angles) polarized BSW. Such angular spectrum has been verified not to change when turning the linear polarization of the excitation beam. We can then assume that the emitting dipoles are isotropically oriented, despite the anisotropic excitation, due to orientational randomization taking place during the molecule permanence in the excited state. Dipoles can

be decomposed in components laying along the 1D-PC surface and perpendicular to it. The first will be coupled both to the TE and TM BSW, the second only to the TM BSW. Therefore the presence of both TE and TM BSW modes allows for an increase of the fluorescence collection efficiency.

In Fig.4 we also plot the theoretically predicted angular spectrum of the fluorescence intensity. The calculations are based on a rigorous Green's function approach [17], where we assumed isotropically oriented emitting dipoles uniformly distributed in a 5 nm thick EtOH layer at the surface of the 1D-PC. In the calculations we assumed for the 1D-PC geometry the thicknesses evaluated from the label-free measurement shown in Fig.2 (left) and the emission spectrum of free Cy7-VG20 in EtOH; we also neglected absorption of the Cy7-VG20 molecules themselves. The matching with the experimental spectrum is rather good, the only fitting parameter being the total emitted energy (the spectra are in arb. un.). The broadening of the experimental peaks is probably due to the broadening of the Cy7-VG20 emission spectrum upon interaction with the 1D-PC surface [18]. We also observe a shift of the TE emission peak towards smaller angles. This is most probably due to re-absorption by the dye molecules themselves of the radiation coupled to the BSW and propagating along the 1D-PC surface before being outcoupled in the TOPAS substrate. We estimate that, for the present 1D-PC design, the leakage length of the TE BSW is in the range of 0.3 mm [19]. In order to give a first qualitative description of the effect, in the inset of Fig.4 we show the angular emission spectra calculated when re-absorption by the Cy7-VG20 is considered. The semi-classical approach used here [17], does not describe accurately fluorescence emission when absorption is also present in the emitting layer. Therefore we assumed absorption in the top 5 nm of the last SiO₂ layer, with the spectrum measured in solution and arbitrary peak increasing values. Passing from the no re-absorption condition (NO ABS) to the case in which the peak extinction coefficient of the 5 nm layer is either 1E-3 (ABS 1X) or 1E-2 (ABS 10X), leads to increasing suppression of the TE BSW fluorescence and shift of the maximum of the angular distribution. Further experimental and theoretical investigations are being carried out to quantitatively describe such effect.

In conclusion we demonstrated here for the first time that BSW optical sensors can be used simultaneously in a label-free and fluorescence mode of operation with the same optical reading configuration, including collection optics and sensing element (CCD). In the label-free mode the sensors show resonance parameters and sensitivity that make the potential LoD twice smaller than equivalent SPP sensors. In the fluorescence operation the emission is efficiently collected and is enough intense to be analyzed by the same CCD sensor. Preliminary measurements show that dyes can be efficiently detected by fluorescence in solutions with a concentration down to 1nM.

Such result is in the stream of studies devoted to the application of photonics crystals for simultaneous label-free and enhanced fluorescence sensing [20,21] aiming at

the smallest possible LoD for a reliable quantitative detection of fluorescent-tagged analytes [22].

This research has received funding from the European Union Seventh Framework Program (FP7/2007–2013) under grant agreement n 318035—Project BILOBA (www.biloba-project.eu) and from the Italian FIRB 2011 NEWTON (grant RBAP11BYNP). The authors acknowledge fruitful discussions with E. Descrovi on fluorescence emission characteristics.

References

- [1] M. Piliarik, J. Homola, *Opt. Express* **17**, 16505 (2009)
- [2] K. Toma, M. Vala, P. Adam, J. Homola, W. Knoll, J. Dostálek, *Opt. Express* **21**, 10121 (2013)
- [3] J. R. Lakowicz, *Analytical Biochemistry* **337**, 171 (2005)
- [4] T. Kosako, Y. Kadoya, H. F. Hofmann, *Nature Photon.* **4**, 312 (2010)
- [5] V. N. Konopsky, E. V. Alieva, *Anal. Chem.* **79**, 4729 (2007)
- [6] A. Sinibaldi, N. Danz, E. Descrovi, P. Munzert, U. Schulz, F. Sonntag, L. Dominici, F. Michelotti, *Sensors and Actuators B* **174**, 292 (2012)
- [7] M. Ballarini, F. Frascella, F. Michelotti, G. Digregorio, P. Rivolo, V. Paeder, V. Musi, F. Giorgis, E. Descrovi, *Appl. Phys. Lett.* **99**, 043302 (2011)
- [8] N. Danz, A. Kick, F. Sonntag, S. Schmieder, B. Höfer, U. Klotzbach, M. Mertig, *Eng. Life Sci.* **11**, 566 (2011).
- [9] S. Kedenburg, M. Vieweg, T. Gissibl, and H. Giessen, *Opt. Mater. Express* **2**, 1588 (2012)
- [10] P. Yeh, A. Yariv, and C.-S. Hong, *J. Opt. Soc. Am.* **67**, 423 (1977)
- [11] P. Rivolo, F. Michelotti, F. Frascella, G. Digregorio, P. Mandracci, L. Dominici, F. Giorgis, and E. Descrovi, *Sens. Actuators B* **161**, 1046 (2012)
- [12] A. Sinibaldi, E. Descrovi, F. Giorgis, L. Dominici, M. Ballarini, P. Mandracci, N. Danz, F. Michelotti, *Biomed. Opt. Express* **3**, 2405 (2012)
- [13] CRC Handbook of Chemistry and Physics, 70th ed. R. C. Weast, ed. (CRC, Cleveland, Ohio, 1989)
- [14] R. Rizzo, N. Danz, F. Michelotti, P. Munzert, A. Sinibaldi, "Limit of detection comparison for surface wave biosensors," *Proc. SPIE* 9141, in press (2014)
- [15] Y. Nagao, T. Sakai, K. Kozawa, T. Urano, *Dyes and Pigments* **73**, 344 (2007)
- [16] N. Barbero, C. Magistris, J. Park, R. Buscaino, C. Barolo and G. Viscardi, submitted (2013)
- [17] N. Danz, R. Waldhaeusl, A. Braeuer, R. Kowarschik, *J. Opt. Soc. Am.* **A19**, 412 (2002)
- [18] T. Baumgaertel, C. von Borczyskowski, H. Graaf, *Nanotechnology*, **21**, 475205 (2010)
- [19] R. Ulrich, *J. Opt. Soc. Am.* **60**, 1337 (1970)
- [20] P. Mathias, N. Ganesh, L. Chan, and B. Cunningham, *Appl. Opt.*, **46**, 2351 (2007).
- [21] F. Frascella, S. Ricciardi, P. Rivolo, V. Moi, F. Giorgis, E. Descrovi, F. Michelotti, P. Munzert, N. Danz, L. Napione, M. Alvaro, and F. Bussolino, *Sensors*, **13**, 2011 (2013).

[22] I. Block, P. Mathias, N. Ganesh, S. Jones, B. Dorvel, V. Chaudhery, L. Vodkin, R. Bashir, and B. Cunningham, *Opt. Express* **17**, 13222 (2009).